Available online at www.sciencedirect.com

ScienceDirect

Procedia CIRP 111 (2022) 296–301

www.elsevier.com/locate/procedia

12th CIRP Conference on Photonic Technologies [LANE 2022], 4–8 September 2022, Fürth, Germany

Pyrometry-based closed-loop control of the melt pool temperature in Laser Metal Deposition with coaxial wire feeding

Christian J. Bernauer[a,*], Avelino Zapata[a], Laura Kick[a], Tony Weiss[a], Martina E. Sigl[a], Michael F. Zaeh[a]

[a]*Technical University of Munich, TUM School of Engineering and Design, Institute for Machine Tools and Industrial Management (iwb), Boltzmannstrasse 15, 85748 Garching, Germany*

* Corresponding author. Tel.: +49 89 289-15568; fax: +49 89 289-15555. *E-mail address: christian.bernauer@iwb.tum.de*

Abstract

Laser metal deposition with coaxial wire feeding is a directed energy deposition process that enables near-net-shape and direction-independent additive manufacturing of metal parts. However, the high sensitivity of the process to disturbances poses a major challenge, as this frequently leads to defective components and rejects. To counteract this, a pyrometer was coaxially coupled into the beam path of the laser processing head to accurately determine the melt pool temperature without limiting accessibility. Applying deterministic test signals, a system model describing the dynamic relationship between the temperature and the laser power was identified. Based on this model, a closed-loop process control was designed. The control system was validated by introducing various disturbances, for which the reference temperature could be tracked with good approximation. The designed temperature control results in reduced effort for tuning the deposition process as well as a lower probability of defects, which saves manufacturing time and cost.

Keywords: laser metal deposition; directed energy deposition; process monitoring and control; coaxial wire feeding; annular laser beam

1. Introduction

Laser technologies are a key factor for establishing additive manufacturing (AM) of metal components in industrial applications. Among the laser-based AM processes, directed energy deposition (DED) techniques offer a number of advantages compared to the widely used processes employing a powder bed. These advantages include the considerably higher deposition rates, the possibility of adding features to existing components, and a high material efficiency.

DED processes using a laser beam as an energy source are also referred to as laser metal deposition (LMD). In these processes, a feedstock material in the form of powder or wire is added to a laser-induced melt pool, enabling material to be deposited in a highly localized manner. While the use of wire offers several advantages such as low cost, good availability, and a clean process environment, it is associated with a high directional dependence due to the typically lateral feeding [1]. However, specialized laser processing heads also enable coaxial feeding of the wire inside an annular laser beam, ensuring directional independence of the process.

Despite the aforementioned advantages, the high sensitivity of the process to disturbances remains a major challenge. Maintaining a constant bond between the wire end and the melt pool requires precisely tuned process parameters, as otherwise typical defect patterns such as "stubbing" or "dripping" can occur [2]. To reduce the effort for extensive parameter studies, process monitoring and control systems are required. An important variable determining the quality of the deposition is the melt pool temperature [3]. If all process parameters remain constant, a heat accumulation typically occurs over time, which is indicated by an increased melt pool temperature. This leads

2212-8271
10.1016/j.procir.2022.08.025

to changes in the process conditions and often to defects. Using a dedicated control system, the heat input into the component can be regulated. To monitor the melt pool temperature, pyrometers and infrared (IR) cameras are commonly used [4]. A well-adjusted and calibrated pyrometer offers the advantage of providing a real-time temperature signal without the additional step of an extensive evaluation of image data.

Various studies investigated the closed-loop control of the melt pool temperature or the highly correlated melt pool width [5]. Salehi and Brandt [6] developed a LabVIEW-based proportional-integral-derivative (PID) controller to track a constant melt pool temperature during powder-based LMD. An in-axis pyrometer was used for monitoring and the process behavior was modeled via a second-order transfer function based on the signals obtained from step inputs to the laser power. It was shown that a closed-loop control stabilizes the process and improves the quality of clad layers. Tang and Landers [3] used an off-axis pyrometer to measure the melt pool temperature in powder-based LMD. A general tracking controller was designed using a first-order transfer function obtained through step response experiments. For constant and time-varying reference temperatures as well as for various process parameter combinations, the controller was found to perform well. However, instabilities appeared for a multi-layer deposition, which was attributed to a lack of information on the prevailing heat transfer characteristics. In order to determine the melt pool width in laser cladding with powder-based LMD, Hofmann et al. [7] used a CMOS camera in conjunction with an image processing algorithm. The laser power was adjusted through a proportional-integral (PI) controller so that the melt pool width was maintained at a constant reference value. As a result, heat accumulation in the part was compensated and the dilution as well as the hardness of the layer showed only minor deviations. A further control system for the melt pool width in powder-based LMD was realized by Akbari and Kovacevic [5] based on an IR camera signal. In the additive build-up, separate first-order system models were determined for the first ten layers to consider changing heat transfer conditions. For each of these layers, an individual PI controller was designed. The control system enabled a more uniform microstructure inside the part than in the case of an uncontrolled process.

For LMD with lateral wire feeding, Heralić et al. [8] developed a PI controller for the melt pool width together with a feedforward compensator for the layer height based on two cameras and a projected laser line. The controller was able to increase the process stability and to reduce droplet formation and stubbing. A similar camera-based control system for LMD with lateral wire feeding was investigated by Gibson et al. [9]. Various control schemes were studied, using the laser power and the feed rate as manipulated variables. The effects of dynamic changes in the main process parameters as well as the resulting bead geometry were examined thoroughly. It was shown that heat accumulation in the component can be exploited to increase the deposition rate without compromising process stability.

While there is a number of studies on thermal control for powder-based LMD, there are only few for the wire-based process variant. For melt pool control in LMD with lateral wire feeding, good results were obtained with camera-based monitoring systems. For LMD with coaxial wire feeding, however, monitoring the melt pool with an in-axis camera is challenging due to the complex beam shaping optics. Instead, an in-axis pyrometer provides a direction-independent solution for measuring the melt pool temperature [10].

The small number of studies on thermal control in wire-based LMD and the lack of studies for the coaxial variant motivated the present work. The objective of this work was, therefore, to investigate the controllability of the existing system with coaxial wire feeding in combination with an in-axis pyrometer. For this purpose, first, the dynamic system behavior was modeled using experimental data. Subsequently, a controller was designed with the help of simulations. The closed-loop behavior of the system was evaluated regarding the performance for reference tracking and disturbance rejection.

2. Experimental setup

The experimental setup is shown in Fig. 1. A 4 kW disk laser (TruDisk 4001, TRUMPF GmbH & Co. KG, Germany) operating in continuous wave (cw) mode generated the laser radiation with a wavelength of 1030 nm. Using a 600 µm optical fiber, the radiation was transmitted to the laser processing head (CoaxPrinter, Precitec GmbH & Co. KG, Germany). Here, the laser beam was shaped in order to allow for coaxial feeding of the wire within an annular beam profile. As a result, a direction-independent LMD process was enabled. An industrial wire feeding unit (DIX FDE PN 100 L, DINSE GmbH, Germany) was used to provide the feedstock. Since the wire was delivered in a coil, its curvature was compensated by a precisely adjusted two-plane wire straightening unit. To move the laser processing head, a six-axis industrial robot (KR 60, KUKA AG, Germany) with a maximum payload of 60 kg was used. The robot was actuated by a robotic control system (KR C4, KUKA AG, Germany).

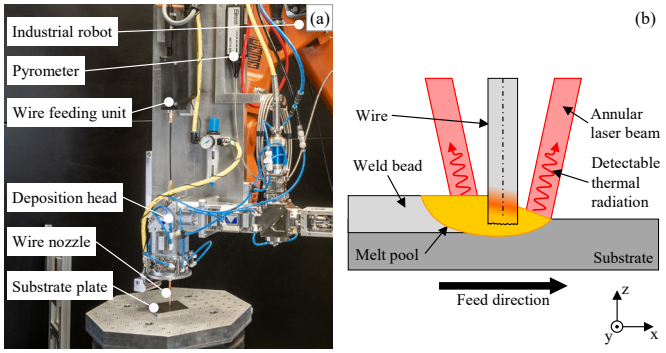

Fig. 1. Laser metal deposition process with coaxial wire feeding: (a) experimental setup; (b) schematic illustration of the process zone

A pyrometer (METIS M322, Sensortherm GmbH, Germany) in one-color mode (sensitive in the range of 1.45 – 1.65 µm) with a temperature measurement range of 600 – 2300 °C was mounted to the laser processing head to coaxially measure the melt pool temperature T_m during the process. The pyrometer was calibrated to measure the surface temperature of the melt pool as described by Zapata et al. [10]. To process the measurement and control signals, a programmable logic controller (PLC) with a sampling rate of 1 kHz was used. The

designed control algorithm was implemented on the internal microcontroller of the pyrometer.

For the experiments, sandblasted plates of austenitic stainless steel AISI 304 (100 mm×100 mm) with thicknesses of 10 mm, 2 mm, and 1 mm were used as substrate material. To remove existing contaminants, the plates were cleaned with isopropanol. The feedstock material was a stainless steel ER316LSi wire with a diameter of 1 mm.

The process parameters, i. e. the laser power P_L, the traverse speed v_t, and the wire feed rate v_w, used for the system identification experiments are discussed in detail in Section 3.1. For the validation experiments, a traverse speed and a wire feed rate of 1 m/min were chosen. During the controlled experiments, the laser power was adjusted by the controller, while a constant laser power of 1500 W was specified for the uncontrolled comparison trials. In all experiments, individual weld beads were deposited directly onto the substrate. A constant shielding gas flow (Argon) of 20 l/min was applied and the focal position was set at −6 mm (below the surface of the substrate), consistent with the setup in [11].

3. Design of the temperature control system

3.1. System identification

In this study, the laser power P_L was used as the manipulated variable since preliminary investigations as well as the literature indicated that it strongly influences the melt pool temperature T_m. In addition, the laser power can be adjusted as required with a very short time delay in the range of a few milliseconds. For the controller design, a model-based approach was favorable. Therefore, a system model describing the dynamic relationship between the laser power and the melt pool temperature was determined via an experimental system identification. Since an exact knowledge of all system states at any time is not required for the controller design, a non-parametric model was applicable.

As shown in Table 1, nine different parameter sets within a stable process window determined in previous investigations [11] were applied. The parameter combinations were chosen so that for three different initial power levels, a high, a medium, and a low energy input per unit length was obtained. Moreover, different bead geometries were realized by varying the ratios between the traverse speed v_t and the wire feed rate v_w. In the experiments, only the given parameters were varied, while all other process conditions were kept constant.

As a deterministic test signal for the excitation of the system, a step increase of the laser power was used. An increase of 500 W was applied after 40 mm during the deposition of single weld beads with a length of 85 mm. At this position, the process had reached its steady state, which means that possible transient effects in the temperature signal resulting from the process start had subsided.

Table 1. Parameter sets used for system identification as well as the resulting initial energy inputs and the speed ratios

Exp. no.	Laser power P_L in W	Traverse speed v_t in m/min	Wire feed rate v_w in m/min	Energy per unit length in J/mm	Speed ratio -
1	1200 – 1700	0.4	1.0	180 – 255	2.5
2	1200 – 1700	1.0	1.0	72 – 102	1.0
3	1200 – 1700	1.6	1.0	45 – 64	0.6
4	1500 – 2000	0.4	1.0	225 – 300	2.5
5	1500 – 2000	1.0	1.0	90 – 120	1.6
6	1500 – 2000	1.6	1.0	56 – 75	0.6
7	1800 – 2300	0.4	1.0	270 – 345	2.5
8	1800 – 2300	1.0	1.0	108 – 138	1.0
9	1800 – 2300	1.6	1.0	68 – 86	0.6

Due to the high melt pool dynamics and the resulting fluctuations in the temperature signal as well as gradual changes due to heat accumulation, particular attention had to be paid to the extraction of suitable data for the mathematical calculation of the system model. For this reason, only the time interval 1000 ms before and after the step increase (a total of 2000 ms) was considered. Due to the short response times of the process, this short interval is sufficient for mapping the dynamic relationship between the laser power P_L and the melt pool temperature T_m.

The system was modeled using a transfer function in the Laplace domain. The estimation of the model parameters based on the trimmed data was performed using the MATLAB System Identification Toolbox. Since a considerable overshoot of the temperature signal occurred in most of the experiments (see Fig. 2), a second-order transfer function with one zero was chosen for the approximation of the system behavior [12]. The transfer function can be described by:

$$G(s) = \frac{Y(s)}{U(s)} = \frac{b_1 s + b_2}{s^2 + a_1 s + a_2} e^{-T_d} \quad (1)$$

Here, T_d is the dead time of the system and b_1, b_2, a_1, and a_2 are unknown coefficients to be determined. The dead time, which can mainly be attributed to communication delays, was experimentally estimated to be 15 ms.

An exemplary temperature signal of experiment 4 is shown in Fig. 2 together with the calculated system model. Increasing the laser power from 1500 W to 2000 W resulted in a steady-state temperature increase of approximately 23 K. The coefficients of the determined transfer functions for all considered parameter sets are given in Table 2.

In order to obtain an overall system model for the parameter range considered, the coefficients of the individual models were averaged following a similar procedure as demonstrated by Meyer et al. [12] and Oakes and Landers [13]. Using an overall model is valid since the deviations for individual parameter sets within the considered range do not represent significant model uncertainties. Thus, the stability of the control loop is not compromised.

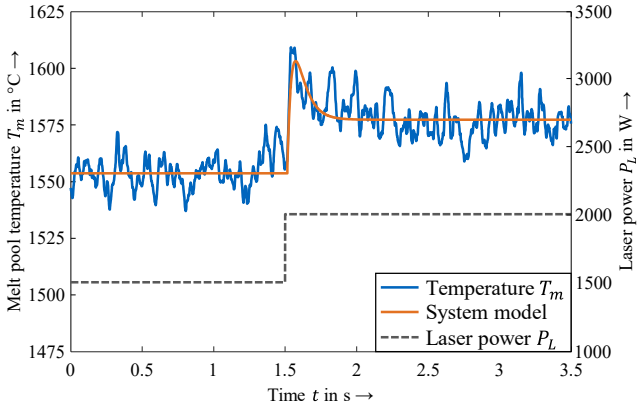

Fig. 2. Measured melt pool temperature for experiment 4 together with the commanded laser power and the corresponding dynamic system model

Table 2. Coefficients of the individual transfer functions for experiments 1 – 9 as well as the calculated mean values applied for the full dynamic process model

Exp. no.	a_1	a_2	b_1	b_2
1	32.60	255.6	3.176	17.93
2	52.79	666.1	0.786	16.44
3	48.64	498.4	3.483	10.06
4	44.84	440.1	5.081	20.78
5	52.38	625.3	3.668	24.05
6	62.91	982.0	4.811	41.33
7	33.53	264.8	2.325	21.07
8	36.89	327.0	4.751	33.10
9	33.62	254.7	2.843	25.79
mean	44.24	479.3	3.436	23.40

The full dynamic process model can thus be expressed by the continuous transfer function $G(s)$:

$$G(s) = \frac{3.436s + 23.40}{s^2 + 44.24s + 479.3} e^{-0.015} \quad (2)$$

Since both existing poles of this transfer function are in the left complex half-plane at $s_1 = -25.29$ and $s_2 = -18.95$, the system can be considered stable. After the system identification, this determined model was used for the model-based controller design.

3.2. Model-based controller design

Using the determined model, the closed-loop system behavior could be investigated via simulations in MATLAB Simulink (R2021a). The fluctuations inherently present in the temperature signal of the LMD process were modeled as a Gaussian distributed noise. For this purpose, the noise signal was superimposed on the output of the controlled system. Moreover, the existing limitations on the manipulated variable due to the finite commandable laser power P_L had to be considered. The closed-loop system is depicted as a block diagram in Fig. 3.

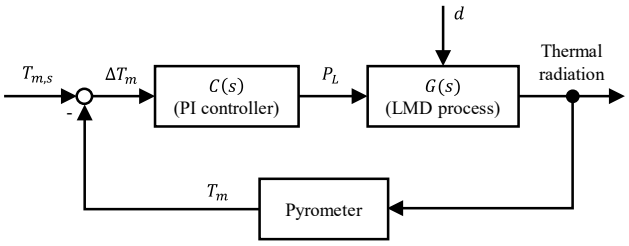

Fig. 3. Block diagram of the employed closed-loop melt pool temperature control system with the temperature setpoint $T_{m,s}$, the control error ΔT_m, and the disturbances d

Since the process could be modeled as a linear time-invariant (LTI) system around the operating point, a PI controller was implemented. A derivative term was not included to avoid instabilities due to the high-frequency noise in the temperature signal. The controller design was carried out using the MATLAB Control System Toolbox.

For the controller tuning, the stability and robustness of the system as well as the dynamic performance were used for evaluation. The controller parameters were chosen so that the controlled signal followed the reference with little to no overshoot and with a low settling time. The steady-state accuracy of the control system was ensured by the integral term in the control algorithm, which corresponds to a pole in the origin of the complex plane for the open-loop system.

A satisfactory dynamic behavior was achieved for a gain K_P of 0.101 and a time constant T_I of 28.4 ms. The transfer function of the controller $C(s)$ in standard form thus is given by:

$$C(s) = K_P \left(1 + \frac{1}{T_I s}\right) = 0.101 \left(1 + \frac{1}{28.4s}\right) \quad (3)$$

In order to examine the performance of the tuned closed-loop control system in the simulation, the temperature setpoint was increased stepwise by 50 K from 1525 °C to 1575 °C. The step response obtained is shown in Fig. 4. The bandwidth of the system is in the range of a few Hertz. As a consequence of that, disturbances such as heat sink changes are effectively compensated for, while the inherent noise does not lead to instabilities.

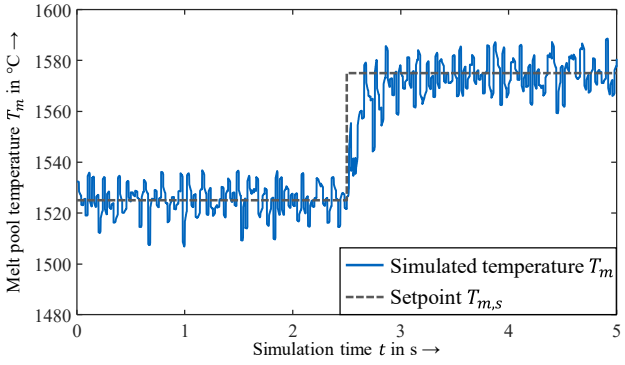

Fig. 4. Performance of the simulated closed-loop control system with a superimposed Gaussian noise for a step change in the reference signal

4. Experimental validation and discussion

In order to investigate the feasibility of the closed-loop control system, various validation experiments were performed in which single weld beads were deposited on the substrate. For all experiments, the data from the first 25 mm and the last 8 mm of the trajectory were excluded to avoid irregularities in the signal resulting from the start and the end phase of the process. In order to quantitatively evaluate the control performance, the standard deviation σ_T of the considered data points in the measured temperature signal was calculated.

For the analysis of the dynamic behavior of the control system during reference tracking, a step increase in the temperature setpoint from 1525 °C to 1575 °C was introduced in analogy to the simulations. The step change was performed on a 10 mm thick substrate plate after a track length of 52 mm. Fig. 5 shows the resulting temperature curve and the commanded laser power P_L. The system demonstrated a satisfactory dynamic performance with a settling time of approximately 0.5 s, whereby no overshoot was apparent. This response is in good agreement with the simulation (see Fig. 4), which indicates that the dynamic behavior was well represented by the system model. It is noteworthy that significant changes in the laser power were performed to adapt the temperature T_m to the reference value $T_{m,s}$. Furthermore, the reference temperature was reliably maintained at both specified levels. In this experiment, the standard deviation was 3.8 K before the step and 4.4 K after the step, corresponding to 0.25 % and 0.27 % of the reference, respectively. In contrast, a standard deviation of 9.3 K was measured for an experiment with a constant laser power of 1500 W.

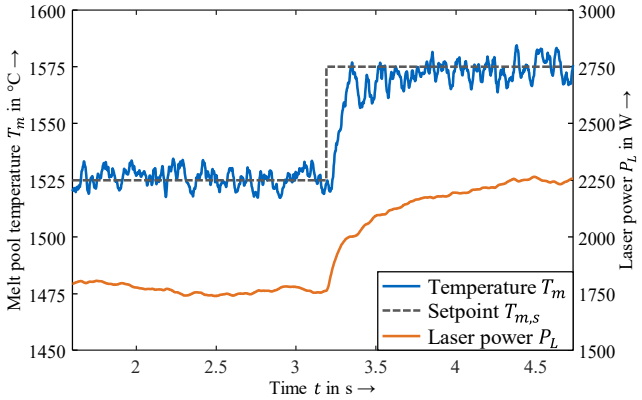

Fig. 5. Performance of the implemented closed-loop control system for a step change in the reference signal together with the laser power commanded by the controller

For a further investigation of the closed-loop system behavior, disturbances in the form of an abrupt change in the substrate thickness were introduced. Transitions from a 10 mm thick substrate plate to a 2 mm thick as well as a 1 mm thick substrate plate after a track length of 81 mm each were investigated. The total length of these weld beads was 160 mm. The reduced heat sink capacity provoked a significant heat accumulation, for the suppression of which the laser power P_L needed to be adapted by the temperature controller. Similar model uncertainties may also occur during the cladding or the additive build-up of complex structures. In Fig. 6, the melt pool temperature T_m and the laser power are plotted for a transition from 10 mm to 2 mm. The mean temperature thereby consistently follows the reference value, whereby the fluctuations on the thin plate are more pronounced. For the constant temperature, a distinct adjustment of the laser power was realized by the controller. It is noteworthy that the laser power is already reduced before the end of the 10 mm plate due to the heat accumulation near the edge.

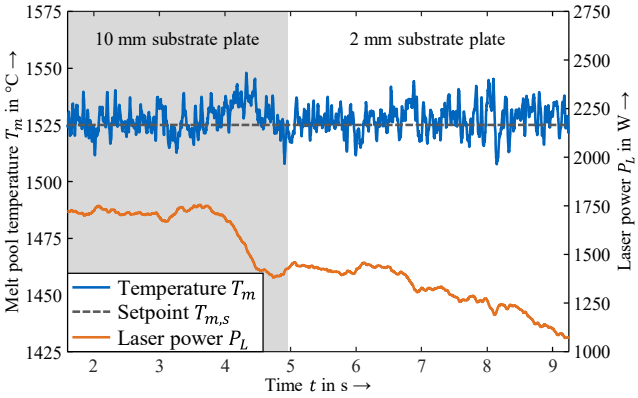

Fig. 6. Closed-loop temperature signal for a sudden change in the substrate thickness from initially 10 mm to 2 mm with a constant setpoint temperature $T_{m,s}$ of 1525 °C

In order to allow for a comparison to the uncontrolled process, analogous experiments were performed using a constant laser power of 1500 W. Table 3 shows the mean laser powers $\bar{P}_L$, the mean temperatures $\bar{T}_m$, and the standard deviations σ_T of the temperature signals during the deposition on the 2 mm and 1 mm plates.

Table 3. Mean values $\bar{T}_m$ and standard deviations σ_T of the temperature signals as well as mean laser powers $\bar{P}_L$ during the temperature controlled deposition on a 2 mm and 1 mm substrate, respectively

Substrate thickness	$\bar{T}_m$ in °C	σ_T in K	$\bar{P}_L$ in W
2 mm	1527.6	6.23	1300.2
1 mm	1525.5	12.72	1271.3

In each case, the mean temperature virtually matched the specified setpoint. Due to the increased heat accumulation, the mean laser power was lower for a thickness of 1 mm than for a thickness of 2 mm. Furthermore, for the controlled process, the standard deviations were lower than for the uncontrolled process with 16.17 K at 2 mm and 15.91 K at 1 mm.

The potential of a temperature-controlled LMD process becomes particularly evident in the experiments with the 1 mm substrate plate. As can be seen in the cross-section in Fig. 7a, during the uncontrolled process, the melt pool penetrated the entire plate due to the high energy input. As a result, melt leaked out on the bottom side of the plate, which also affected the geometry on the top side. In contrast, the temperature control prevented an excessive energy input and, thus, through-welding by significantly reducing the laser power, as shown in Fig. 7b.

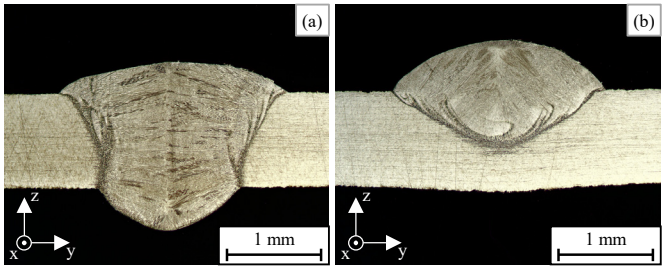

Fig. 7. Deposition on a 1 mm substrate plate: (a) uncontrolled process with a constant laser power of 1500 W; (b) controlled process with a constant melt pool temperature of 1525 °C

The experiments carried out demonstrate that a stable and robust control of the melt pool temperature in LMD with coaxial wire feeding is feasible. For the further application of the closed-loop control, however, the assessment of task-dependent reference temperatures as well as appropriate limits of the commanded laser power must also be considered. In a wire-based process, the feedstock has to be fully melted at all times in order to maintain stability without the defect patterns of stubbing or dripping [2]. For this reason, the laser power must not fall below a particular threshold value. While this was less relevant in the validation tests conducted, it can be particularly critical when building large components since the transition from a 3D heat conduction mode directly on the substrate plate to a 2D heat conduction mode, especially in thin walls, leads to increased heat accumulation. It may, therefore, no longer be possible to achieve the desired temperature value without causing an unstable process. Thus, for the additive build-up of multi-layer parts, wire-based LMD requires a detailed understanding regarding the range of suitable temperature setpoints that can be achieved in a stable manner depending on the process conditions. This subject will be investigated in more detail in a subsequent study.

5. Conclusions

In this work, a control system for the melt pool temperature in laser metal deposition with coaxial wire feeding was developed and investigated in detail. The inline temperature measurement was performed via an in-axis pyrometer. A series of step response experiments covering a wide range of process conditions was conducted and a second-order system model describing the dynamic relationship between the laser power and the melt pool temperature was identified from this. Based on the determined model, a proportional-integral controller was designed to robustly track the desired reference temperature without any steady-state deviation. The control system was validated regarding the tracking performance for an abruptly changing reference value. Furthermore, disturbances in the form of a varying substrate thickness could be effectively compensated, illustrating the high robustness of the closed-loop system.

In future work, the challenges of temperature controlled LMD when building multi-layer parts will be investigated in detail. Thereby, a well-defined specification of the melt pool temperature will help to increase the reliability of the process and thus promote its further industrial application. In this context, the microstructural and mechanical properties of the components built while using the temperature control system will also be evaluated thoroughly.

Acknowledgments

The results presented were achieved within the AdDEDValue project, which is supported by the German Federal Ministry for Economic Affairs and Climate Action (BMWK) within the funding program “Digitalization of Vehicle Manufacturers and the Supplier Industry” (contract number 13IK002L) and supervised by the VDI Technology Center (VDI TZ). We would like to thank the BMWK and the VDI TZ for their support and for the effective and trusting cooperation. Furthermore, we would like to thank our partners Precitec GmbH & Co. KG, Sensortherm GmbH, and DINSE GmbH for providing the systems used.

References

[1] Kotar M, Fujishima M, Levy GN, Govekar E. Advances in the understanding of the annular laser beam wire cladding process. J. Mater. Process. Technol. 2021;294: pp. 1–12.
[2] Motta M, Demir AG, Previtali B. High-speed imaging and process characterization of coaxial laser metal wire deposition. Addit. Manuf. 2018;22: pp. 497–507.
[3] Tang L, Landers RG. Melt Pool Temperature Control for Laser Metal Deposition Processes – Part I: Online Temperature Control. J. Manuf. Sci. Eng. 2010;132: 1–9.
[4] Tang Z-J, Liu W-W, Wang Y-w, Saleheen KM, Liu Z-c, Peng S-t, Zhang Z, Zhang H-C. A review on in situ monitoring technology for directed energy deposition of metals. Int. J. Adv. Manuf. Technol. 2020;108: pp. 3437–3463.
[5] Akbari M, Kovacevic R. Closed loop control of melt pool width in robotized laser powder–directed energy deposition process. Int. J. Adv. Manuf. Technol. 2019;104: pp. 2887–2898.
[6] Salehi D, Brandt M. Melt pool temperature control using LabVIEW in Nd:YAG laser blown powder cladding process. Int. J. Adv. Manuf. Technol. 2006;29: pp. 273–278.
[7] Hofman JT, Pathiraj B, van Dijk J, Lange DF de, Meijer J. A camera based feedback control strategy for the laser cladding process. J. Mater. Process. Technol. 2012;212: pp. 2455–2462.
[8] Heralić A, Christiansson A-K, Ottosson M, Lennartson B. Increased stability in laser metal wire deposition through feedback from optical measurements. Opt. Lasers Eng. 2010;48: pp. 478–485.
[9] Gibson BT, Bandari YK, Richardson BS, Henry WC, Vetland EJ, Sundermann TW, Love LJ. Melt pool size control through multiple closed-loop modalities in laser-wire directed energy deposition of Ti-6Al-4V. Addit. Manuf. 2020;32: pp. 1–13.
[10] Zapata A, Bernauer C, Hell M, Zaeh MF. Studies on the direction-independent temperature measurement of a coaxial laser metal deposition process with wire. Lasers in Manufacturing Conference 2021: pp. 1–9.
[11] Zapata A, Bernauer C, Stadter C, Kolb CG, Zaeh MF. Investigation on the Cause-Effect Relationships between the Process Parameters and the Resulting Geometric Properties for Wire-Based Coaxial Laser Metal Deposition. Metals 2022;12: pp. 1–16.
[12] Meyer SP, Bernauer CJ, Grabmann S, Zaeh MF. Design, evaluation, and implementation of a model-predictive control approach for a force control in friction stir welding processes. Prod. Eng. 2020;14: pp. 473–489.
[13] Oakes T, Landers RG. Design and implementation of a general tracking controller for Friction Stir Welding processes. American Control Conference 2009: pp. 5576–5581.